IEEE Access
Multidisciplinary ⋮ Rapid Review ⋮ Open Access Journal

Received June 1, 2021, accepted June 22, 2021, date of publication June 25, 2021, date of current version July 5, 2021.

Digital Object Identifier 10.1109/ACCESS.2021.3092696

Multi-Terminal HVDC System With Offshore Wind Farms Under Anomalous Conditions: Stability Assessment

AHMED E. B. ABU-ELANIEN[1], (Senior Member, IEEE), AYMAN S. ABDEL-KHALIK[1], (Senior Member, IEEE), AND AHMED M. MASSOUD[2], (Senior Member, IEEE)

[1]Electrical Engineering Department, Faculty of Engineering, Alexandria University, Alexandria 21544, Egypt
[2]Department of Electrical Engineering, Qatar University, Doha, Qatar

Corresponding author: Ahmed E. B. Abu-Elanien (ahmed.abuelanien@alexu.edu.eg)

This work was supported by the National Priorities Research Program (NPRP) through the Qatar National Research Fund under Grant 9-092-2-045. Open Access funding was provided by the Qatar National Library.

This work did not involve human subjects or animals in its research.

ABSTRACT Droop control is widely adopted to control Multi-Terminal high-voltage Direct Current (MTDC) systems with offshore wind farms. During permanent faults, the faulty line should be isolated promptly to preserve a high reliability of the MTDC system. This paper examines the MTDC system performance following a faulty line outage. This study aims to identify the outage types that may lead to a complete loss of system voltage stability and the outages that may have a secondary effect on the system. Moreover, strategies for dealing with outages that may lead to a complete shutdown of the system are also presented. Furthermore, the ranges of droop gains' values that can be employed following fault occurrence to preserve system transient stability are studied. Different scenarios are explored during faulty conditions such as surplus and sparsity of wind power, line overcurrent, outage of lines connected to wind farms, and outage of lines connected to AC grids to validate this study. MATLAB/Simulink platform has been employed to elucidate the presented concept.

INDEX TERMS Droop control, HVDC, MTDC, stability, wind energy.

I. INTRODUCTION

Offshore wind farms' share in the worldwide power generation is estimated to increase due to their richness in clean power [1], [2]. Therefore, special consideration is given to wind energy as a primary power source in the European super grid [1], [3]. Voltage source converter-based Multi-terminal high-voltage Direct Current (MTDC) grids are the main platform to collect generated wind energy [1]–[3]. They link offshore wind farms with different AC grids via both overhead lines and submarine cables. Voltage source converter-based MTDC systems have several advantages, such as low power losses, the ability to include long DC cables, and the capability to connect asynchronous systems. Nevertheless, MTDC network faults may severely affect converters' semiconductor devices due to the fast rise of fault current to high levels [3]–[6]. Accordingly, DC faults should be detected, and the faulty line should be isolated in a few milliseconds to protect the converter semiconductor devices. Fast line isolation can be achieved via high-speed electronic circuit breakers [5], [7]. However, the faulty line's isolation should be followed by a suitable adjustment in the control system to maintain stability and safe operation of the MTDC system. Otherwise, the system may experience severe overvoltage, overcurrent, excess power losses, or surplus wind power. Moreover, a complete system loss may occur if corrective actions are not taken [8], [9].

Droop control is an effective technique to control MTDC systems [1], [10]–[12]. Power-sharing can be controlled, employing droop gains, which are always selected to preserve safe power flow. Moreover, a better droop control design leads to optimal power flow in the MTDC system [8], [13]–[16]. Nevertheless, in fault conditions, the droop gains should be updated during outages to ensure a safe power-sharing among different terminals/lines [8], [9], [17]. While the droop gains' adaptation can avoid voltage and current violations, the MTDC system's stability needs to be studied to assure that the

The associate editor coordinating the review of this manuscript and approving it for publication was Ali Raza.

system restores its stable operating state during post-fault adjustments.

Droop control adjustment during converter outage is highlighted in [9]. The needed droop control design for optimum operation during line and converter outages is presented in [8]. However, the MTDC system voltage stability after modifying the droop gains lacks a comprehensive investigation. Moreover, in case of system instability, the needed corrective action to restore the system to its normal operation state was not discussed. Furthermore, the risky and non-risky outages are not identified. The AC side's frequency stability following an outage in MTDC networks is studied in [18]–[20]. Nonetheless, this research studied the AC side stability, while the DC side's voltage stability has not been investigated. Small signal stability analysis of DC side of MTDC system is investigated in [21]–[24] with varying control parameters, operating conditions, line resistance, and inductance of current limiting reactor. However, these studies are focused on healthy condition only. The voltage stability of the DC network following a faulty condition is not studied. The DC side stability is studied in [11] and [25] under AC fault conditions. Nevertheless, the effect of DC faults is not studied despite its notable effect on the MTDC network stability and power balance. Moreover, the AC side fault effect on the MTDC network is not high enough due to the power converter's control and protection. Evaluation of power reserves of MTDC converters to overcome power mismatch during converter outages is investigated in [26]. However, introducing a power reserve in a converter increases its rating, which is not an economic solution to overcome DC voltage fluctuation due to power mismatch. AC damping torque analysis method is applied in [27] to test the DC voltage oscillations in MTDC networks. However, the voltage oscillations represent a real problem in AC networks. However, the DC voltage oscillations is not a common problem in MTDC networks.

This paper presents a DC side stability study following a faulty condition in MTDC systems with offshore wind farms. This paper's first objective is to identify the risky outage types that may lead to a complete breakdown of the system and the non-risky outages that have a secondary effect on the system. Besides, strategies for dealing with risky outages are also presented. The second objective is to identify the safe range of the droop gain values that can be used in the reconfigured system for different outage conditions due to different faults. Different power mismatch scenarios are addressed in this study, such as surplus and sparsity of wind power injections. Moreover, different types of line outages leading to different post-fault configurations are considered. The main contributions in this paper can be bulleted as follows:

- The MTDC system performance following the disconnection of a line due to DC fault is investigated to study power, voltage, or current violations.
- The risky and non-risky outage types inside the MTDC system are differentiated.

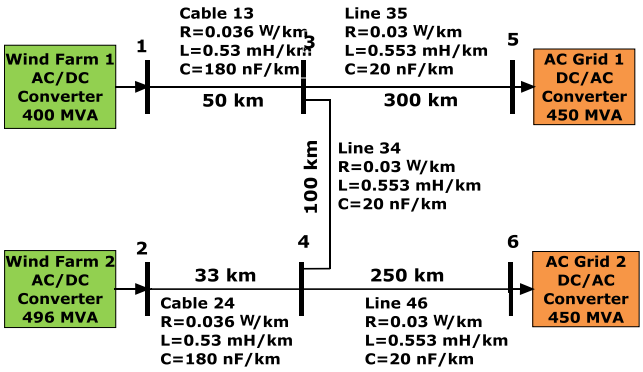

FIGURE 1. MTDC model.

- The required subsequent corrective actions to maintain system voltage stability and optimum operation due to any risky outages are presented.
- The safe range of droop gains to guarantee safe transient response of the reconfigured MTDC system during outage conditions under minor disturbances is also assessed. Eigenvalues are evaluated with a wide range of droop gains for the reconfigured system after the faulty line's disconnection. This safe range represents the allowable droop gains range to keep reconfigured system transient stability under marginal operational condition changes.

II. MTDC POWER SYSTEM MODEL

In this section, the MTDC power system model is introduced. Without loss of generality, a radial MTDC example is considered for clarification. Fig. 1 shows a typical 6-bus, 500 kV(±250 kV), bipolar MTDC system with two offshore wind farms [8]. In this system, the wind farms' electrical power is transmitted to shore via two submarine cables (cable 1-3 and cable 2-4). The wind power is then transmitted to two AC grids using three overhead lines (lines 3-4, 3-5, and 4-6). All lines are conventional bipolar HVDC lines. The rated power of the wind farms and the AC grids, the line parameters, and the line lengths are depicted in Fig. 1. The rated power levels of the wind stations are 400 MVA and 496 MVA, respectively. The two AC grids' powers are 450 MVA. Therefore, in normal operation, the AC grids can receive the total injected wind power at rated conditions. The power-sharing in all lines is governed utilizing adaptive droop control. The current capacities for submarine cables 1-3 and 2-4 are 800A and 1000A, respectively. All overhead lines have the same current capacity, which is 900A. These line capacities ensure no overcurrent during normal operation. Line parameters are indicated in Fig. 1.

A simulation model is built using MATLAB/SIMULINK under the Sim Power Systems toolbox to carry out the intended stability study. The built-in line and cable models are employed in this simulation model. To avoid long simulation time, an average modeling approach has been employed to simulate the power converter. The grid-side converters are controlled using DC voltage controllers under

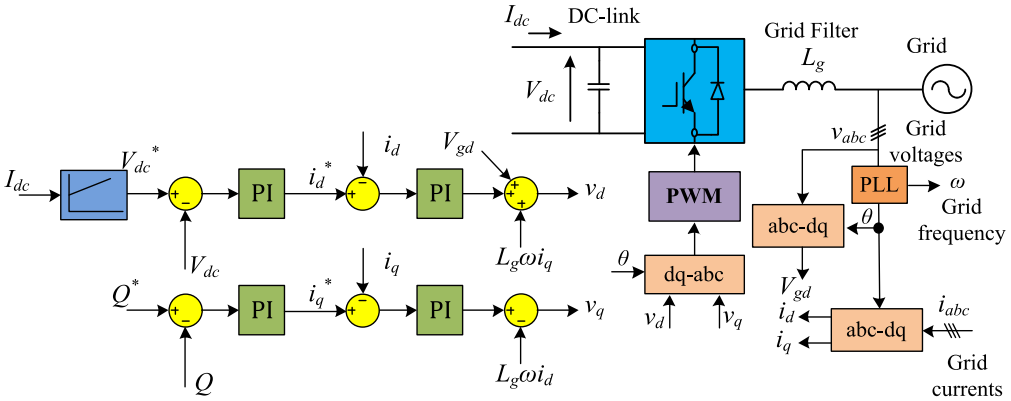

FIGURE 2. DC voltage control mode of the grid-side converter.

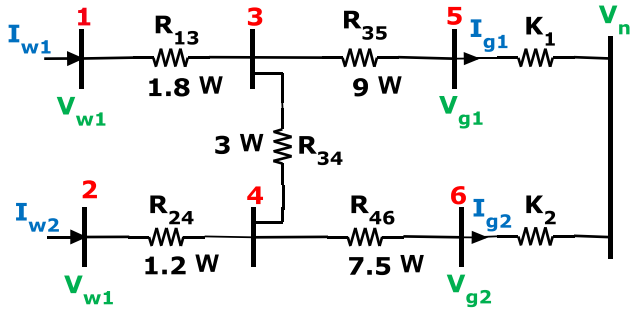

FIGURE 3. Equivalent DC circuit of the MTDC model.

power-sharing [28], where each converter is controlled using two nested control loops. The inner loop controls the dq current components of the AC line currents, where the quadrature current component controls the reactive power components injected into the grid, while the reference direct current component is found based on an outer control loop that controls the DC-link voltage magnitude, as shown in Fig. 2. The required voltage decoupling terms are calculated based on the grid angular frequency ω and the grid interfacing inductance Lg. The wind-side converters are simply simulated by dependent current sources based on the desired injected wind power.

III. OPTIMAL DROOP GAINS FOR MTDC SYSTEM

Optimal droop control showed success in controlling MTDC systems during different operational modes [8], [13]–[16]. In optimal droop control, the gains are calculated based on the system configuration and operational conditions. To evaluate the droop gains, the system equivalent circuit should be obtained. Fig. 3 shows the DC equivalent circuit for the system shown in Fig. 1.

A droop gain of a grid-side converter can be represented by a virtual resistance K. The general relation between the converter terminal voltage and input current can be calculated as follows based on the showed current directions

$$V_n = V_{gi} - K_i i_{gi} \tag{1}$$

where,

V_n: the system base voltage (1 pu);

V_{gi}: the i^{th} grid-side converter terminal voltage;

i_{gi}: the i^{th} grid-side converter current.

In optimal droop control, the gains should be re-calculated for any change in the wind power injection to ensure global optimum operation. To calculate the optimal droop gains, bus voltages are maximized, within the allowable limits, to reduce the line currents and accordingly reduce power losses. An optimization function is used to solve for optimal droop gains [16], [19]. Other research work developed different methods to obtain the optimum droop gains without solving the optimization problems [8], [14], [15], [29].

In case of a fault in the MTDC system, the faulty line should be isolated to keep the system operational. Following the faulty line's disconnection, the grid-side converters' optimal droop gains should be re-calculated according to the new reconfigured system [8]. In this regard, optimum droop gains are calculated for every change in the injected wind power, considering the system's new configuration as explained in [8]. In this paper, the optimal gains for the reconfigured system after faulty line disconnection are calculated according to the technique developed in [8]. However, even if the optimal droop gains are re-adjusted according to the new system configuration, the system stability may be affected due to other reasons, including the following:

- The calculated optimum droop gains may be outside the safe droop gains range to guarantee the reconfigured system's transient stability under small disturbances. In order to check the transient stability of the reconfigured system under small disturbances, eigenvalues study should be done.
- A significant power mismatch between the injected wind power and the consumed AC side power is likely to create voltage instability.

Two stability studies are needed in this regard. The first is the droop gains' safe margins allowed for the reconfigured MTDC system after the disconnection of the faulty line. The second is the voltage stability of the reconfigured system. The safe range maintains the system transient stability under small operational disturbances like changes of wind power injection. Any change of injected wind power requires

a change in the droop gains, which should be inside the safe range to operate safely and optimally if possible. If the updated droop gains are outside the predetermined safe range, the system may suffer from transient instability, or large oscillations, which may lead to another outage. Studying the system eigenvalues will lead directly to these safe margins that maintain the transient system stability during the period of droop gains change. This study depends only on system configuration and parameters. The eigenvalues analysis is illustrated in section IV.

The usage of the droop gain's safe margins does not guarantee system voltage stability under outage conditions. The safe range of droop gains has nothing to do if the power mismatch due to the outage is large, or if the wind power should be dropped to zero due to wind line outage. The type of the outage, the system loading condition, and level of wind power injections may lead to loss of system voltage stability even if the used droop gains are within the safe limit. Accordingly, the second study is the system voltage stability following various outages under different loading conditions and wind power injections. Section V includes this study. Moreover, the risky and non-risky outage types of the MTDC will be identified. Accordingly, in order to have a complete stability study of the DC side of the MTDC under anomalous conditions, the reconfigured system needs to first overcome the power mismatch of the injected /consumed power due to the outage to ensure voltage stability. After overcoming this issue, the droop gains should be within the safe limit indicated to guarantee the reconfigured system's stable operation under small disturbances.

In this work, the line connected to any wind farm is called the wind farm line. Line 1-3 and line 2-4 in the MTDC model are examples of wind farm lines. The line connected to a grid-side converter, such as line 3-5 and line 4-6, is termed a grid line. Any other line is designated as an interconnecting line.

IV. SYSTEM TRANSIENT STABILITY

A. ANALYSIS OF SYSTEM EIGENVALUES

Voltage Source Converters (VSCs) as two-level converters and Modular Multilevel Converters (MMCs) can be employed in MTDC systems. In this paper, the two-level VSC is assumed to simplify the simulation model for such a large system. However, in converters such as MMCs, the dynamics of the internal state variables can be neglected assuming well-regulated MMC, where the order of the MMC model can be reduced to first-order similar to that in [30]. The time constant of this reduced-order model can be assumed small (namely, the current control loop); hence the presented concept can be employed.

Typically, the VSC dynamics can be approximated where the fast transient of the VSC sub-systems VSC can be neglected through setting several assumptions such as the converter harmonics are negligible, the inner current control loop is much faster than the outer control loops, VSC losses are neglected. Nevertheless, it can be assumed that the outer control loop (either active power control or dc voltage control) has a long time constant that is considered long to affect the presented system model transient. Therefore, the model dynamics of the VSC can be neglected in this study.

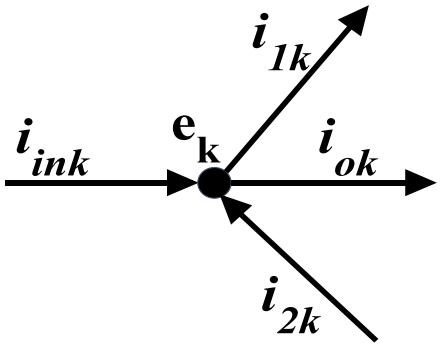

FIGURE 4. The currents at an arbitrary node *k* in the MTDC system.

The MTDC system typically consists of several nodes and branches (irrelevant of the connection type). There are three types of nodes; power input nodes, power output nodes, and intermediate nodes. Please consider a general node shown in Fig. 4. Generally, the currents at any node k can be expressed, using KCL, as follows:

$$C_k \dot{e}_k = \alpha_k i_{ink} - \beta_k i_{ok} + \sum_{j=1}^{j=l_k} \gamma_{jk} i_{jk} \tag{2}$$

where;

C_k: is the total effective capacitance at this node (that considers the cable(s) model and the converter capacitors).

e_k: is the voltage at node k.

α_k and β_k are constants that take the values 1 and 0, respectively, at power input nodes (i_{ink} for the wind-side converter), and take 0 and 1, respectively, at power output nodes (i_{ok} for the grid-side converter).

l_{jk}: is the total number of branches at this node.

γ_{jk}: is a constant that takes 1 and -1 when the current direction is into and out of node k, respectively.

The voltage across a branch j can be expressed as follows:

$$L_{jk} \frac{di_{jk}}{dt} = \left(e_j - e_k\right) - R_{jk} i_{jk} \tag{3}$$

where i_{jk} is the current through a branch jk (between nodes j and k) with an equivalent inductance of L_{jk} and resistance of R_{jk}.

e_j and e_k are the voltages at nodes j and k, respectively.

In the case of n-terminal HVC network with l_{jk} branches, the state-space model can be expressed as follows:

$$\begin{aligned} \dot{X} &= AX + BU + MW \\ Y &= CX \end{aligned} \tag{4}$$

where X is the system states $X = [X_1 X_2]^T$, $X_1 = [e_1, \ldots, e_{n1}]^T$, and $X_2 = [e_{n1+1}, \ldots, e_{n1+n2+n3}, i_1, \ldots, i_l]^T$

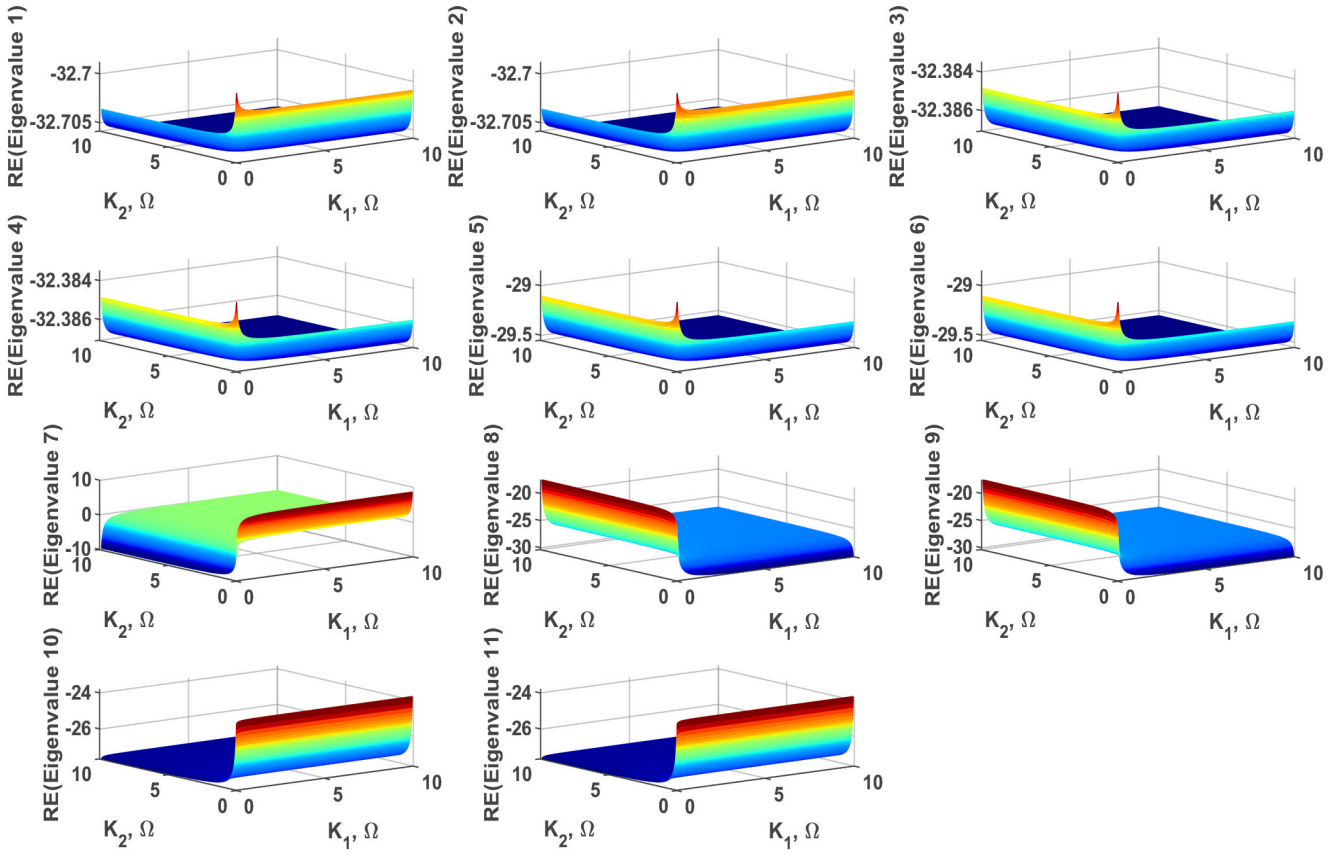

FIGURE 5. Effect of changing droop gains on the MTDC system's dynamic stability (i.e., real parts of the system eigenvalues).

n_1 is the number of output nodes, n_2 is the number of input nodes, and n_3 is the number of intermediate nodes.

$$U = \left[i^*_{o1}, \ldots, i^*_{o\_n1}\right]^T, \quad W = \left[i^*_{in1}, \ldots, i^*_{in\_n2}\right]^T \text{ and}$$
$$Y = [X_1 \quad 0]^T.$$
$$A = \begin{bmatrix} 0 & A_{12} \\ A_{21} & A_{22} \end{bmatrix}, \quad B = \begin{bmatrix} B_1 \\ 0 \end{bmatrix}, \quad M = \begin{bmatrix} 0 \\ M_2 \end{bmatrix}, \text{ and}$$
$$C = \begin{bmatrix} I & 0 \end{bmatrix}$$

where I is the identity matrix, and A_{12}, A_{21}, A_{22}, B_1, and M_2 are obtained from the MTDC network similar to that in [6].

To design the droop control gains at the grid-side converters (output nodes), stability should be ensured. The droop control gains' main objective is to maintain the DC voltage constant irrespective of system disturbances (e.g., wind power changes, wind-side converter(s) outage) throughout output feedback control. The droop control gains can be obtained through the following relation.

$$U = -KX \tag{5}$$

where K is a diagonal matrix of $n \times n$, therefore, the state-space model can be expressed as follows:

$$\dot{X} = (\text{A-BK})\, X + MW \tag{6}$$

System stability can be studied throughout the eigenvalues of the system, which can be expressed as follows:

$$\det(sI - (\text{A-BK})) = 0 \tag{7}$$

The state-space model for the MTDC network shown in Fig. 1 is elucidated in Appendix A. Based on system parameters given in Fig. 1, the variation of the system eigenvalues as a function of the gain matrix K calculated based on (7) are given in Fig. 5, where the gains K_1 and K_2 are varied up to 10 Ω. Fig. 5 shows that the eigenvalues may attain a positive real part in case of having a low value of K_1 or K_2. This is clear in eigenvalues 5, 6, and 7 in Fig. 5. In case of proper selection of K_1 and K_2 (taking into consideration the resistance of the grid lines), system eigenvalues with a negative real part will be guaranteed therefore ensuring system stability over the relevant range of the droop gains K. Based on Fig. 5, the droop gains can be changed safely. Nevertheless, attaining low values for the droop gains might affect system stability. Furthermore, the droop gains' safe range is affected by the resistances of the connected grid lines. In Appendix A, the droop gains' safe range that maintains system stability is illustrated under different grid lines' resistances. The values of R_{35} and R_{46} have been increased by a factor of 10 then decreased by factor 10 to study the effect of gridline resistance on the safe and stable range of the droop gains. Based

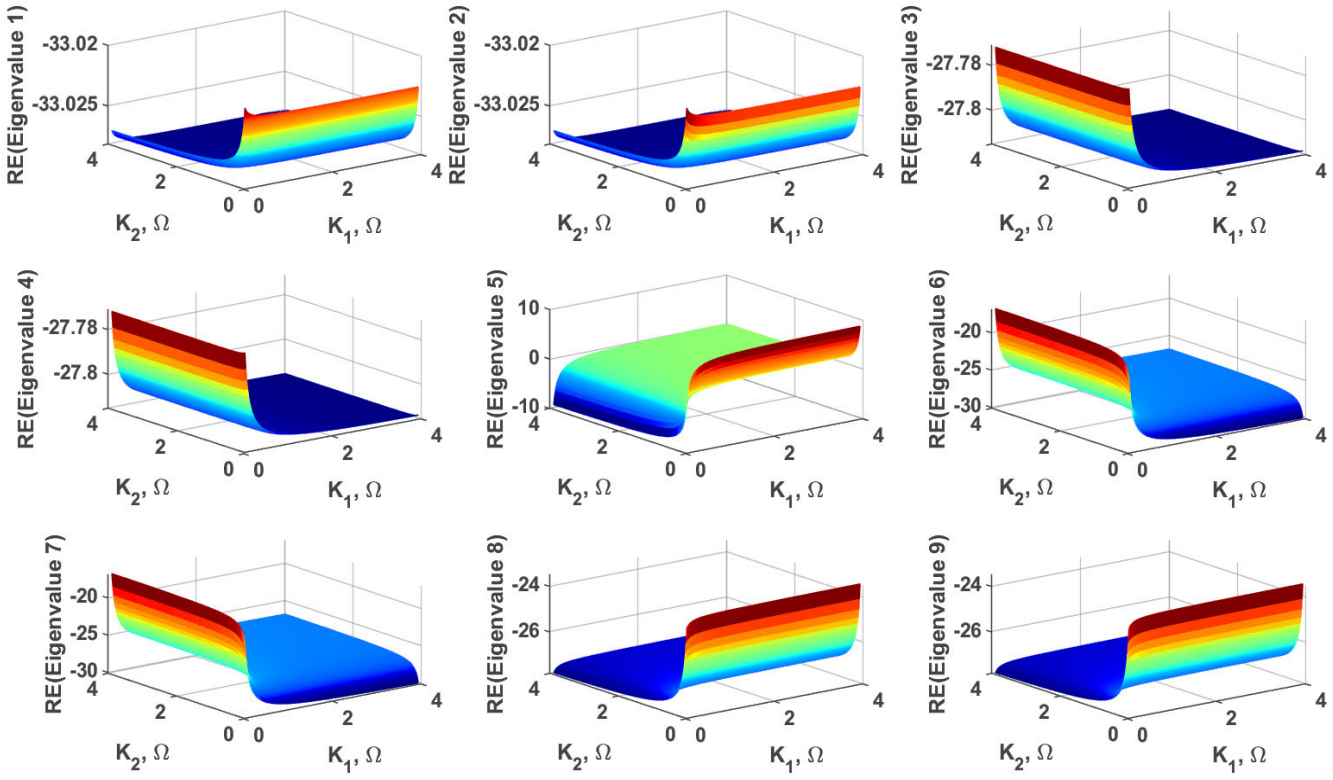

FIGURE 6. Relation between droop gain values and real parts of the system eigenvalues after disconnection of line 1-3.

on this study, for higher grid line resistances, the lowest values of droop gains that ensure proper dynamic stability are higher, and vice versa. For the studied system, it was found that a droop gain larger than unity is not likely to yield any positive eigenvalues, which means a stable system operation. This range is for the studied system mainly. The droop gains' safe range may be affected by MTDC system parameters and topology. The aforementioned general steps can be used to find the droop gain safe ranges for different topologies.

B. SAFE RANGE OF DROOP GAINS UNDER FAULTY CONDITIONS

This section provides a safe range of droop gains under different fault conditions to maintain the system transient stability. The presented study here depends on the system configuration after isolating the faulty line. In fault conditions, isolation of the faulty line reconfigures the MTDC system. Considering a fault in each MTDC line, the droop gains' safe range will be studied separately. Figs. 6 to 9 show the effect of variation of the droop gains on the eigenvalues under different reconfigurations due to a permanent fault in one of the lines. Fig. 6 elucidates the system stability through the relationship between the droop gains and the eigenvalues' real parts, considering the MTDC system with line 1-3 disconnected due to a fault. The system state-space model can be derived directly from Appendix A by removing rows 3 and 7, and columns 3 and 7 from matrix A, then rearranging accordingly matrices B, C, and D.

The effect of disconnecting line 2-4 has been similarly addressed in Fig. 7. It can be noticed from Figs. 6 and 7 that the stability of the MTDC system is maintained throughout the entire range except at low values of droop gains (typically less than one). The disconnection effect of line 3-5 is investigated in Fig. 8, where the relationship between droop gain K_2 and real parts of the eigenvalues is depicted. It can be noticed that the system stability is maintained at a droop gain of 20 or higher. Fig. 9 portrays the effect of line 4-6 disconnection. It can be concluded that the real parts of the eigenvalues are maintained negative for a droop gain larger than unity.

V. SYSTEM VOLTAGE STABILITY DURING FAULTY CONDITIONS

The safe limits of the droop gains for transient stability were introduced in the previous section. Although from the connectivity point of view, the used droop gains range is safe, the system loading and wind injection may lead to system voltage instability. This section discusses the voltage stability of the MTDC system during and after a faulty condition under different operating scenarios.

The outage of a wind farm line, grid line, and interconnection line are tested under different wind power injections. The necessary actions needed to maintain the system stability

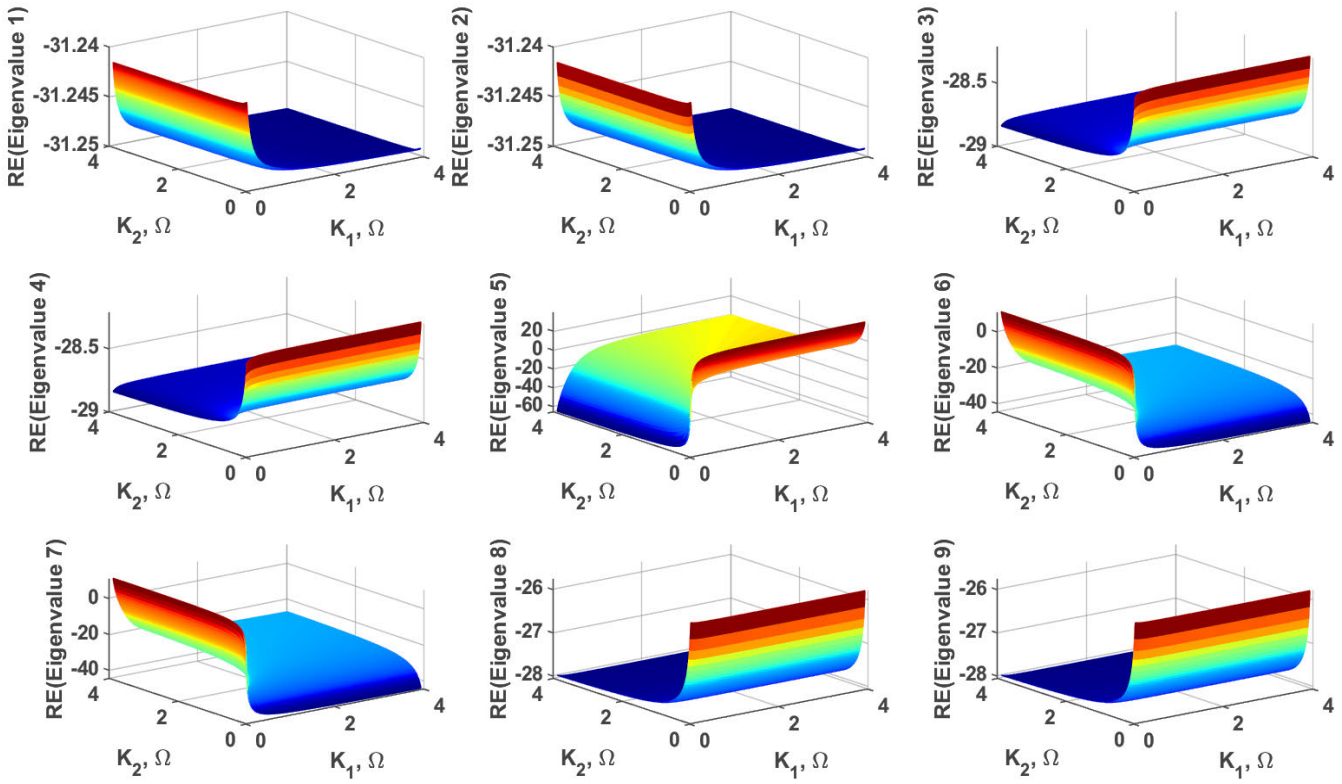

FIGURE 7. Relation between droop gain values and real parts of system eigenvalues after disconnection of line 2-4.

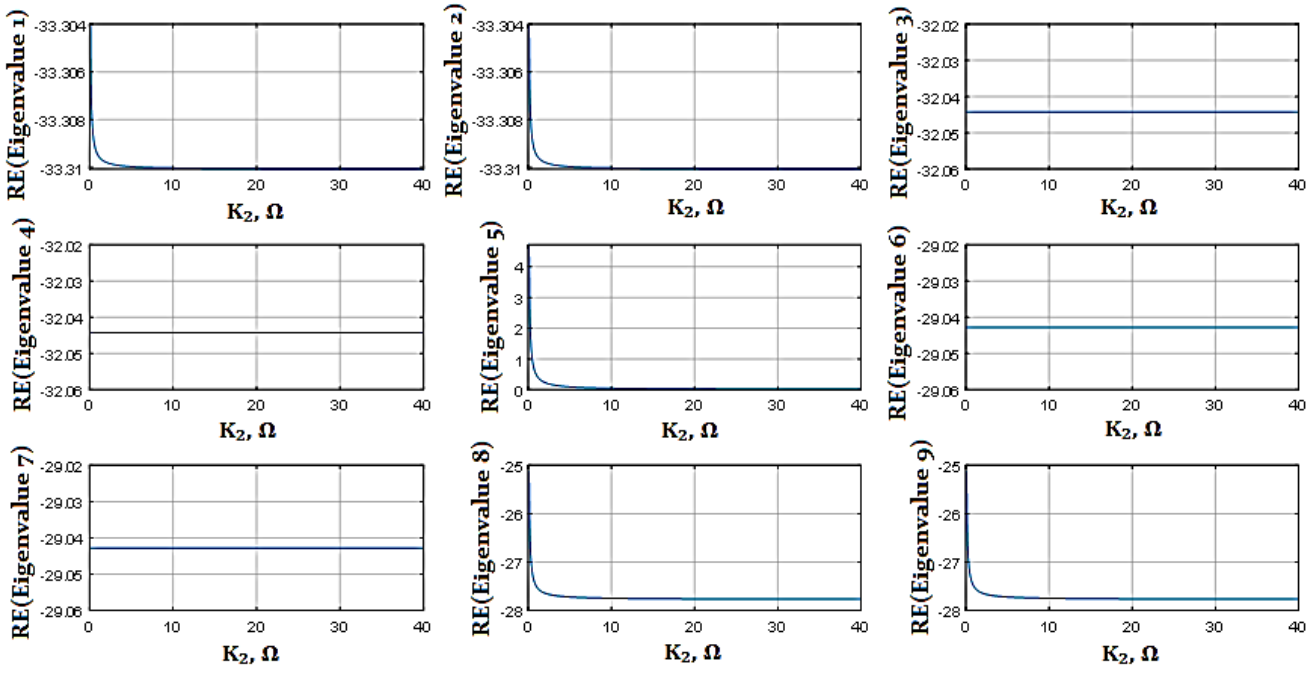

FIGURE 8. Relation between droop gain value and system eigenvalues after disconnection of line 3-5.

after faulty conditions are investigated. The optimal droop gains before and after fault are calculated according to [8].

The system dynamic performance is investigated using a MATLAB/SIMULINK model with the system parameters

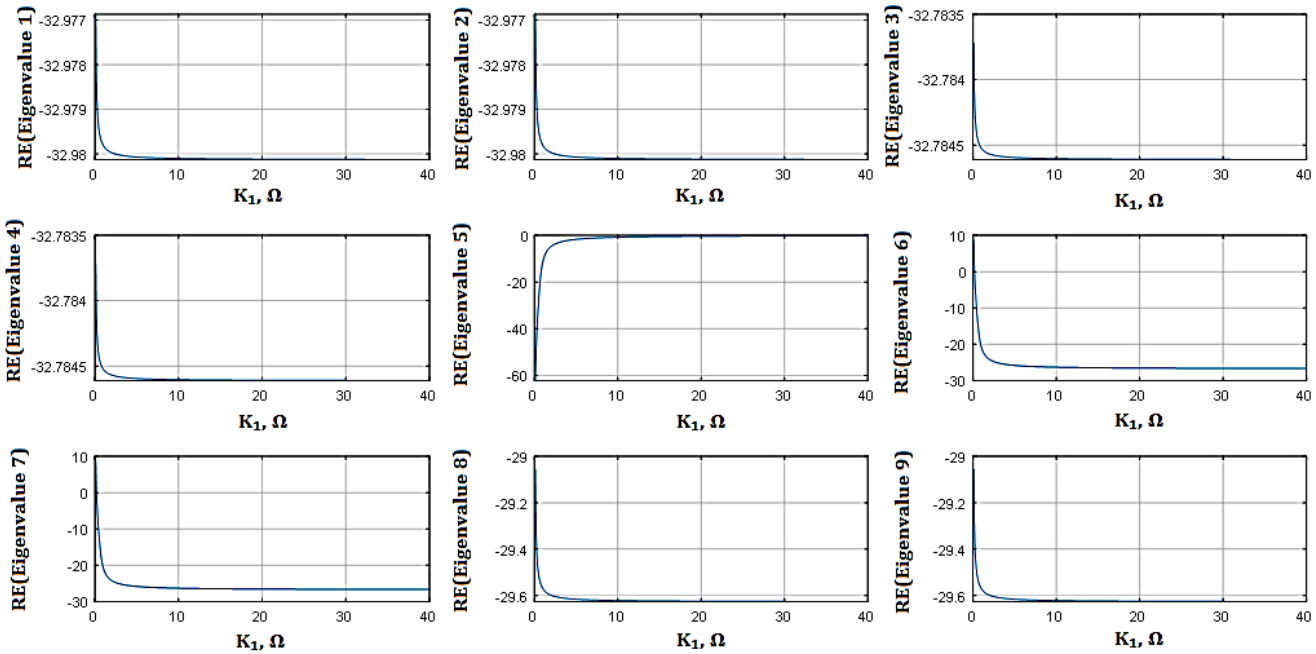

FIGURE 9. Relation between droop gain value and system eigenvalues after disconnection of line 4-6.

shown in Fig. 1. The wind farm is modeled using a current-controlled current source. Each wind farm is equipped with a shunt Chopper-Controlled-Resistor (CCR). CCR is automatically activated in emergencies to avoid steep voltage rise under sudden significant power imbalance [31].

In the next subsections, the system dynamic performance is studied for disconnection of the grid line 3-5 under different wind power injections, disconnection of wind farm line 1-3, and disconnection of interconnection line 3-4. The maximum permissible voltage is taken as 1.05 pu (the base voltage is 500 kV) [8], [14]. The maximum permissible line current is equal to its respective rating, as shown in Fig. 1.

A. OUTAGE OF GRID LINE WITH LOW WIND POWER INJECTION

This section studies the effect of grid line outage. In this case study, line 3-5 outage is used to represent this type of outage.

A permanent fault is simulated in line 3-5. The pre-fault wind powers P_{w1} and P_{w2} are assumed as 207 MW and 115 MW, respectively. Accordingly, the total generated wind power is much lower than the wind farms' total rated power. It is also much lower than the total power of the AC grids' converters. A step increase in P_{w1} and P_{w2} is assumed at 1s, as shown in Fig. 10. Under these wind injections, the two grid-side converters' optimum droop gains to minimize system losses are found to be $K_1 = 61.6$ and $K_2 = 57.8$, respectively [8]. According to the eigenvalues study, these values will not initiate transient stability problems. Consequently, the optimum pre-fault wind farm voltage V_{w1} becomes 1.05pu, the maximum permissible voltage, whereas V_{w2} stabilizes at 1.047 pu, as shown in Fig. 10 (c). Wind farm 1 has the highest wind power injection; accordingly, it is logical to have the highest voltage, which leads to lower current and power losses. More information about the optimum operation of the MTDC systems can be found in [8], [14], [15], [29]. Terminal currents before fault inception are shown in Fig. 10(a) and (b). Fig. 10(b) is a zoomed view of Fig. 10(a). The pre and post-fault bus voltages are shown in Fig. 10(c). It can be noticed that the pre-fault terminal currents and voltages are below the maximum allowable values, which are the current rating for each line and 1.05 pu for voltage.

A permanent fault is simulated in line 3-5 at 3s. Then 4 ms after fault inception, the fault is cleared by the protection system (1 ms for relay decision and 3 ms for complete isolation) [32]. Fig. 10(a) shows that terminal currents during fault conditions jumped abruptly to high levels due to the discharge of converters' smoothing capacitors [33]. The currents fall to new values after clearance of the faulty section. It can be noted from the zoomed view in Fig. 10(b) that grid 1 current falls to zero due to isolation of the faulty line 3-5. The remaining terminal currents fall to new values due to the change in the system configuration. The new values of the currents are below the maximum capacity of their respective lines. Accordingly, the line currents are not expected to affect the system.

After the disconnection of line 3-5, while the same droop gains are maintained at their pre-fault values, and the same injected power is preserved, the injected wind power is transmitted totally to the grid through line 4-6. Since the droop gains do not change after disconnecting the faulty line, the 1.05pu voltage constraint is violated, as shown

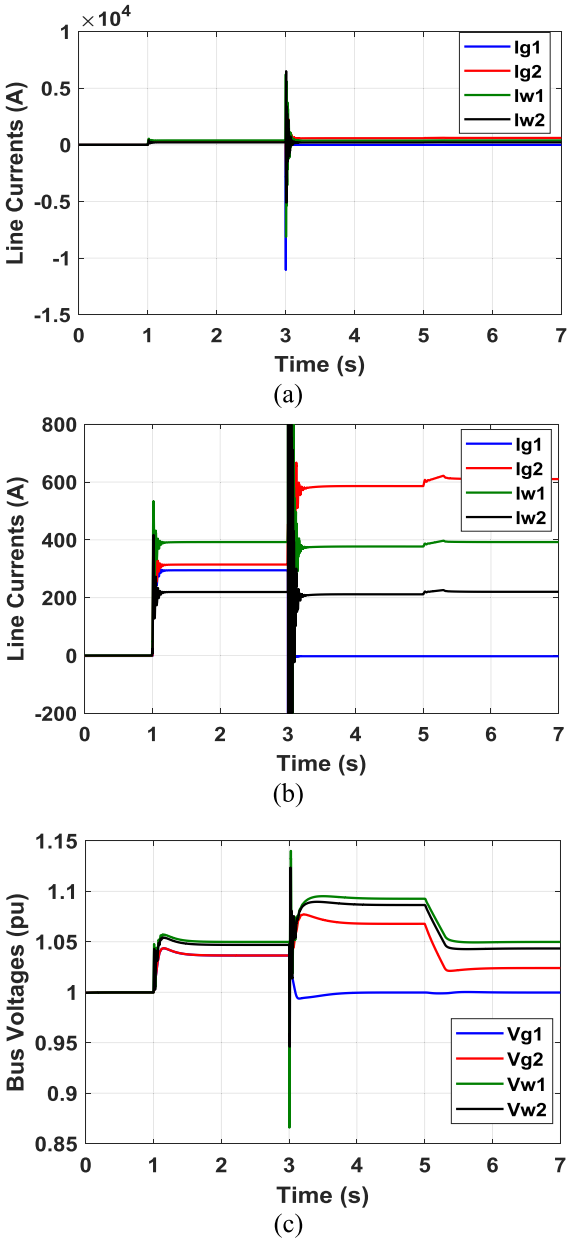

FIGURE 10. Dynamic study during disconnection of line 3-5 at low wind power injection (a) terminal currents, (b) zoom on terminal currents (c) bus voltages.

in Fig. 10 (c), which entails reducing the grid-side converter's droop gain connected to line 4-6 to avoid system overvoltage. For the same injected power and applying the presented technique in [8], the new value of the optimum droop gain at grid-side converter 2 is $K_2 = 19.65$. Since this value is smaller than the safe value for transient stability, which is 20, K_2 is updated to 20.

At 5 s, K_2 is changed to 20; hence, all bus voltages are reduced. The bus voltage with the highest magnitude, V_{w1}, is reduced to its maximum value near 1.05pu because K2 is not exactly at the optimum value (19.65). The line currents are slightly increased due to voltage reduction. The bus voltage, V_{g1}, ceases to 1pu, which represents the system voltage under no-load.

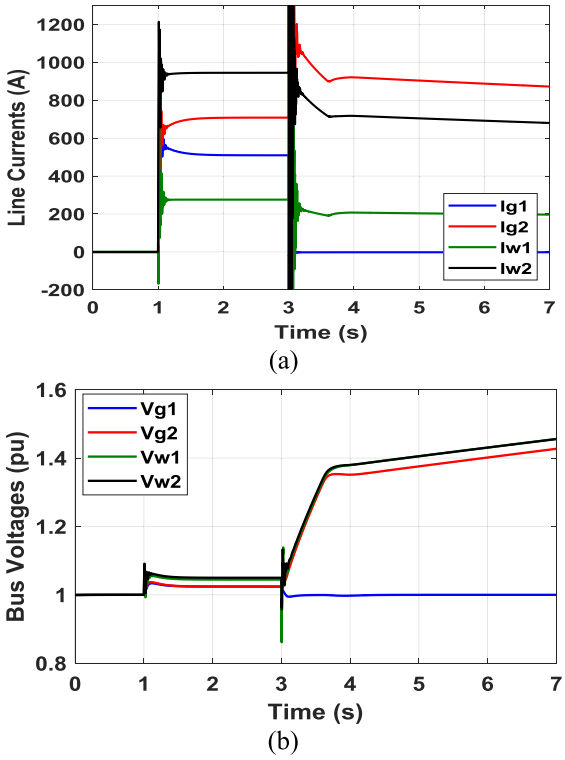

FIGURE 11. Dynamic study during disconnection of line 3-5 at high wind power injection with no CCR system (a) terminal currents (b) terminal voltages.

The presented study shows the challenge of maintaining the droop gains without change after system reconfiguration due to faulty conditions. As depicted in Fig. 10(c), the healthy converters' voltages have been changed to high levels after line disconnection. These voltage values may severely affect the MTDC if not reduced to safer values. Moreover, the voltage protection system may disconnect the system unnecessarily to avoid this overvoltage. The MTDC system stabilizes typically following the faulty line disconnection and droop gain change for this operational scenario. Although system voltage increases to a maximum of nearly 1.09 pu after a faulty line disconnection, it is restored to its safe limits again after adjusting the droop gain K_2 to its new safe value. This slight overvoltage cannot be assumed loss of stable system operation. Accordingly, no extra elements, circuit, or control system is needed to retain the system's dynamic stability.

B. OUTAGE OF GRID LINE WITH HIGH WIND POWER INJECTION

A permanent fault is again simulated in grid line 3-5. However, the pre-fault wind power injections are assumed to be of higher values: $P_{w1} = 144$MW and $P_{w2} = 496$ MW. At 1 s, a step increase in wind power is assumed for wind farms 1 and 2, as shown in Fig. 11. The optimum droop gains employed in this case are $K_1 = 23.74$ and $K_2 = 17.05$. According to the eigenvalues study, these values maintain healthy system transient stability. At 3 s, a fault is simulated in line 3-5; accordingly, the line is disconnected using fast-acting circuit

breakers after 4 ms like the previous case. Since the capacity of the line connected to grid 2 (line 4-6) is now violated, the power unbalance drives the system voltages to increase; accordingly, the whole system becomes unstable. Moreover, the value of K_2 is lower than the safe range to guarantee transient stability for this fault (K2 is needed to be larger than 20). To avoid this problem, the total injected wind power should be reduced to preserve the power balance between wind farms and grid 2. Calculations based on [8] show that system power balance can be restored, and optimal operation can be obtained if the input wind powers P_{w1} and P_{w2} are reduced to 94.5 MW and 378 MW, respectively. The optimum droop gain for the second grid-side converter is calculated as $K_2 = 10.86$. However, this droop gain cannot guarantee the system's transient stability after the faulty line's disconnection. Therefore, the droop gain should be increased to 20 to maintain transient stability.

The power reduction of the wind turbines is carried out through pitch control. Since this control technique is relatively slow because it includes mechanical actions, the huge unbalance between the high input wind power and grid 2 power capability will increase system voltages to high unstable values, as shown in Fig. 11(b). Accordingly, the whole MTDC system is lost even with reducing the injected wind power to the system. Even with the change of droop gain to the updated safe value at 3s, the system voltage continues to run away, and system stability is entirely lost, as shown in Fig. 11 (b). It is worth mentioning that the overvoltage protection of the MTDC system trips the whole system before reaching these high voltage values.

In this case, a chopper-Controlled-Resistance (CCR) [34], [35] system is essential to avoid wind turbine disconnection during a fault condition. The CCR is inserted across the converter DC link for a short period until the pitch control is activated. The shunt CCR is a constant resistor connected in series with a chopper circuit to control the average current in the constant resistor; hence the average dissipated power can be varied. Therefore, after line 3-5 disconnection during high wind power injection, both pitch control and CCR systems are immediately enabled. The pitch control reduces the power to the updated safe value. At the same time, the CCR systems are enabled for both wind farms to facilitate safe line currents and regulated terminal voltages at 1.05pu, as shown in Fig. 12(a) and Fig. 12(b). It is assumed that the pitch control takes a 2s period to reduce the injected wind power to the new desired levels. The CCR systems are automatically disconnected after a full reduction of the wind power to the updated safe values. It is worth mentioning that the added CCR during the transient period changes the system topology during this transient period. The CCR resistors add more transient stability to the system. Accordingly, the safe range of the droop gains changes to be any value larger than unity. At 5 s, the droop gain K_2 is updated to its optimal value (10.86) to ensure optimum power transmission. This optimal droop gain does not cause any transient problem, although it is less than 20. The reason for that is the existence of

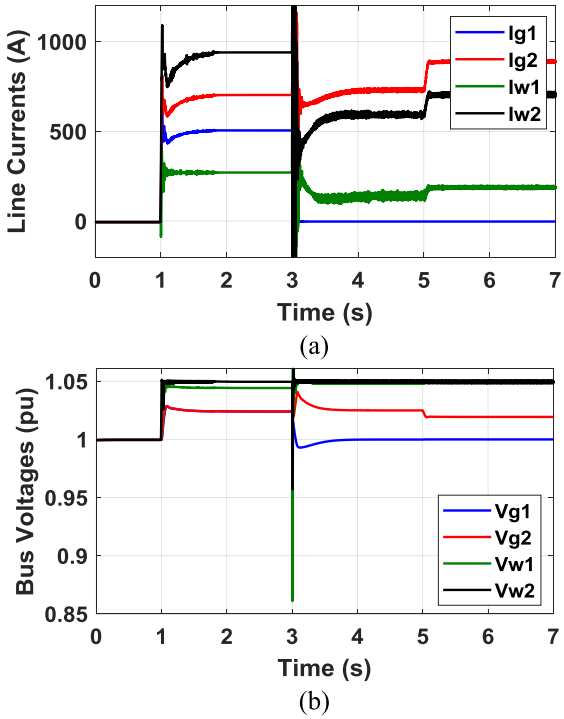

FIGURE 12. Dynamic study during the disconnection of line 3-5 at high wind power injection with CCR system (a) terminal currents (b) terminal voltages.

the CCR in the transient period. The CCR is disconnected after the transient period. The CCR circuits are disconnected due to reduced injected wind power and DC link voltage. The droop gain value of 10.86 will not create a transient instability problem after CCR disconnection. This is because the transient instability problem arises at the time of change in the droop gain; however, in this case, the droop gain was already updated to 10.86 before CCR disconnection.

Fig. 12(a) shows that the line currents did not violate the maximum capacities after fault occurrence. However, the current values are not optimal. Following a change of the droop gain K_2 to its updated optimal value, the optimum wind farms' currents become 180A and 720 A, respectively, which summed up to 900A in grid line 2-4. These currents ensure the system's optimum operation as they are inversely proportional to the lines' resistances [14], [15]. Fig. 12(b) shows that the wind farm voltages are controlled to a safe level of 1.05pu after fault condition due to the existence of CCR. Following a change of the droop gain K_2, both voltages of wind farms are continued at 1.05 pu due to operation with optimum droop gains. The operating voltage of grid 1 is 1 pu due to the disconnection of power injection to the grid-side converter. Additionally, the grid 2 voltage is within the safe limit.

Based on the abovementioned study, the system's stability, in this case, is not guaranteed by just isolating the faulty line and changing the droop gains. The wind farm control should reduce the wind power injections to lower values that guarantee safe and optimal operation. The high wind power injections cause dangerous voltage instability, and the

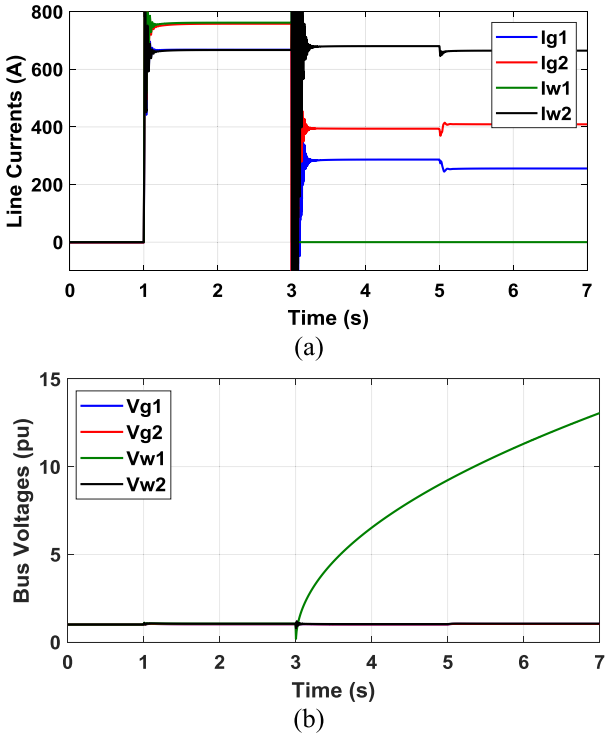

FIGURE 13. Dynamic study due to disconnection of line 1-3 without CCR system (a) terminal currents (b) terminal voltages.

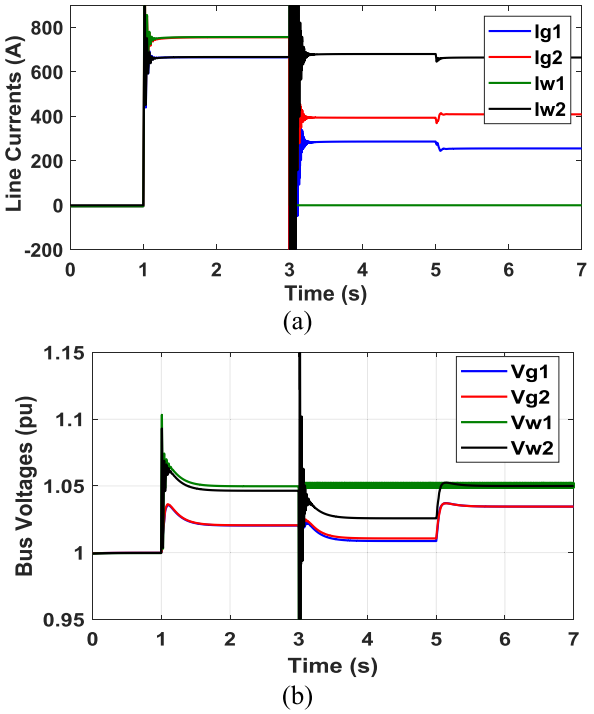

FIGURE 14. Dynamic study during the disconnection of line 1-3 with the CCR system (a) terminal currents (b) terminal voltages.

probability of losing the whole system increases. However, the CCR system is intended to absorb the excess wind power after faulty line isolation. The CCR system limits the voltage to a safe value of 1.05 pu during the faulty period. It is disconnected from the system after the reduction of wind power to the new optimal safe values.

C. OUTAGE OF WIND FARM LINE

In this case study, line 1-3 outage is used as an example to illustrate wind farm line outage. A fault is simulated in the wind farm line 1-3. Subsequently, the line is disconnected after 4 ms by the protection system. For high or low power injection, if the injected power P_{w1} is maintained at the same pre-fault level, V_{w1} starts to increase dramatically. Therefore, the CCR protective system should be enabled to limit the voltage increase by bypassing this surging power until the turbine pitch control reduces the wind power to zero. The power injected by the second wind turbine through line 2-4 is transmitted to the grid and shared by the grid lines 3-5 and 4-6. The pre-fault wind farm injected powers are assumed to be $P_{w1} = 400$MW and $P_{w2} = 349$ MW. The optimal pre-fault droop gains are $K_1 = 15.26$ and $K_2 = 13.58$. Since these values are higher than unity, the system transient stability is preserved. The pre-fault line currents and bus voltages are shown in Fig. 13. It can be noticed that the system was working optimally and stably before the fault.

Following the faulty line disconnection, wind farm 1 is suddenly exposed to the no-load condition. Accordingly, the wind power injection of farm 1 should be reduced to zero using the pitch control. The same situation as the previous sub-sections appears here. The control system takes some time to reduce the blade angle to ensure no wind power injection. Consequently, the wind farm voltage jumps to an extremely high level, as shown in Fig. 13(b). Even if the droop gains are changed, the voltage increases to a high unstable value if no CCR system exists. If the wind farm voltage is not controlled during this period, the wind farm should be tripped out of service to avoid damage. To control the wind farm voltage increase following the faulty line's isolation, the same CCR system should be activated to provide a path for the wind power until the reduction of injected power to zero. Therefore, the wind farm bus voltage does not exceed the maximum allowable voltage (1.05 pu).

The terminal current distribution and bus voltages are shown in Fig. 14 with the CCR system. It is clear from Fig. 14(a) that the terminal currents are below the line current capacity even after faulty line isolation. However, the line currents are not optimized until the droop gains are optimized based on the new system configuration. The bus voltages are in the safe range after a faulty line disconnection. The bus voltage of wind farm 1 is limited to 1.05 pu after faulty line disconnection with the aid of the CCR system, as shown in Fig. 14(b). After 2 s from the line disconnection, the CCR system is disconnected, and the droop gains are adjusted to their new optimized values to ensure optimal operation of the new reconfigured system. The new droop gains are found to be 67.51 and 42.2, respectively. As illustrated in Fig. 6, these values do not cause any transient instability.

Fig. 14(b) indicates that the bus voltage of wind farm 2 increases to 1.05 after droop gain adjustment, reflecting the

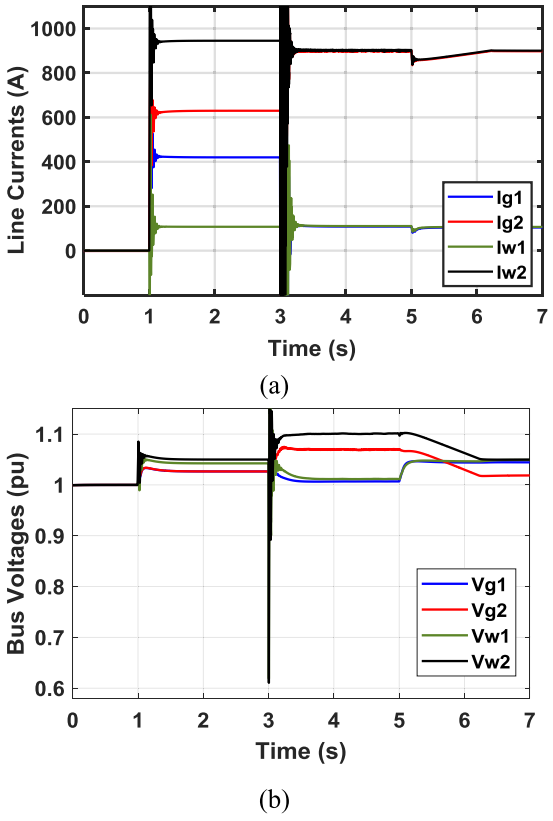

FIGURE 15. Dynamic study during disconnection of line 3-4 (a) terminal currents (b) terminal voltages.

system's optimal operation due to reducing the line currents and transmission losses. The bus voltage of wind farm 1 is kept at 1.05 pu using the CCR system. After the CCR system's disconnection, the voltage is still at 1.05 pu, the no-load voltage.

In the case of low wind injection, the same approach is followed because the grid-side converters can absorb the wind power at any level. Moreover, the problem of increased wind farm voltage exists for any value of wind injection. Therefore, the CCR system should be activated upon wind farm line fault until the wind arm power is reduced to zero. The droop gains should also be re-adjusted after reducing wind farm power to maintain optimum operation and avoid any line overload.

D. OUTAGE OF AN INTERCONNECTING LINE

The system voltage stability due to an outage of an interconnecting line is studied in this section. A fault is simulated in line 3-4 at 3 s. The pre-fault wind powers are assumed as follows: $P_{w1} = 56$ MW and $P_{w2} = 496$ MW. Fig. 15 shows terminal voltages and line currents before and after the outage.

The system was working optimally before fault at droop gains of $K_1 = 31.5$ and $K_2 = 21$. Transient stability is preserved using these values. The outage of line 3-4 splits the MTDC system into two separate sub-systems. The post fault line currents are still within safe limits, as shown in Fig. 15 (a). Moreover, the grid and wind line currents become identical due to the outage of the interconnecting line. Fig. 15 (b) indicates that the V_{w1} and V_{g1} are within safe limits. However, V_{w2} and V_{g2} violate the maximum permissible voltage. The sudden increase in I_{46} due to the outage of line 3-4 together with the high wind power injection of the second wind farm leads to an increase of V_{w2} and V_{g2} to 1.1 and 1.07 pu, respectively. To restore the safe operation of wind farm 2, its power should be reduced to 472.5 MW to keep the line current at a rated value of 900A with V_{w2} at a maximum value of 1.05 pu. The optimum droop gain K_2, in this case, is 10.38. Fig. 15 shows the voltage and current of wind farm 2 and grid 2 after adjusting the power and droop gain at 5 s. Although the system connecting wind farm 1 by grid 1 is safely operated; however, it is not optimal. At 5 s, the droop gain K_1 should be changed to 212.71 to restore the optimal operation of wind farm 1. After the droop gain change, the wind farm voltage is maximized to 1.05 pu, and the line currents are minimized, as shown in Fig. 15(b). After the outage of line3-4, the system is divided into two two-terminal simple systems. The safe droop gain range of each of them is above unity. The used drop gains values are completely safe since it is larger than unity.

Unlike the outage of the wind farm line or outage of the grid line at high wind power injection, the outage of an interconnecting line is not likely to create severe instability conditions. The reason is that the wind farm lines and grid lines are designed to carry the system current at any wind power injection, even during the outage of any interconnecting line. Moreover, the outage of an interconnecting line does not cause any converter isolation, which is the main reason for the uncontrolled increase in system voltage. Therefore, the interconnecting line's outage may create disturbances in voltages and currents; however, these disturbances can be disconnected with droop control adjustment.

A comparison between the main outage scenarios for the studied system is depicted in Table 1. This table summarizes the droop gains ranges for all types of outages. It is worth mentioning that these values are based on the used MTDC model. For any other system, the safe ranges of droop gains under different outage conditions could be found using the systematic steps explained in the Appendix. From the table, it can be concluded that high wind power injection is one of the main reasons for hazardous outages. The outage of a wind farm line or a grid line under high wind penetration is likely problematic. Moreover, the wind farm line's outage is more likely to create a loss of voltage stability. The least problematic outage is the outage of the interconnecting line. The outage that produces the disconnection of a converter is likely to produce a voltage instability problem. To avoid the voltage instability problem, a CCR should be installed in the wind farm converters. Since the fault type may be any kind, a CCR should always be installed in the wind farm converters to consume any extra wind power during fault and limit the voltage to a maximum of 1.05 pu.

TABLE 1. Comparison between different outage cases for the studied system.

Outage type	System status after an outage	Transient stability study	Voltage stability study		
		Droop gain range for transient stability	Minor operational problems	Major voltage instability	Need for CCR
Wind farm line	Injected wind power < AC grid absorption capability	Any value >1	Not likely	Yes	Yes
Grid line with low wind power injection	Injected wind power < AC grid absorption capability	- Any value >20 for an outage of line 1-3 - Any value >1 for an outage of line 4-6	possible	No	No
Grid line with high wind power injection	Injected wind power > grid absorption capability	- Any value >20 for an outage of line 1-3 - Any value >1 for an outage of line 4-6	Not likely	Yes	Yes
Interconnecting line	Injected wind power ~= AC grid absorption capability	Any value >1	possible	Not likely	No

VI. CONCLUSION

The stability of MTDC systems under abnormal conditions was studied. A typical six-bus MTDC model is used to facilitate this study. The following points can be concluded from the study.

1. The safe range of droop control gains can be changed when the system configuration changes due to a faulty line's disconnection. The safe range of droop gains guarantees system transient stability during the change of droop gains process under marginal operational disturbances. The system eigenvalues analysis is used to identify this range. It was found that transient instability is likely to occur for low values of droop gains. However, The correct safe range of droop gains to maintain transient stability can vary from a system to another; therefore, each system should be studied separately to evaluate these safe ranges.
2. In the case of grid line outage during low wind power injection, the droop gains should be re-adjusted to the optimal values to ensure safe and optimal operation of the MTDC system. No severe voltage instability condition is expected for this outage type.
3. Wind power should be reduced for grid line outage during high wind power injection to cope with the new MTDC grid power capability. An unstable increase in the systems voltage is expected after removing the faulty line. A CCR circuit, connected in parallel with the DC capacitor of the wind farm converter, should be activated to avoid an uncontrolled increase of the system voltage during the outage. The CCR system

$$\begin{bmatrix} e_5 \\ e_6 \\ e_1 \\ e_2 \\ e_3 \\ e_4 \\ i_{13} \\ i_{24} \\ i_{34} \\ i_{35} \\ i_{46} \end{bmatrix}^{\circ} = \begin{bmatrix} 0 & 0 & 0 & 0 & 0 & 0 & 0 & 0 & 0 & 1/C_5 & 0 \\ 0 & 0 & 0 & 0 & 0 & 0 & 0 & 0 & 0 & 0 & 1/C_6 \\ 0 & 0 & 0 & 0 & 0 & 0 & -1/C_1 & 0 & 0 & 0 & 0 \\ 0 & 0 & 0 & 0 & 0 & 0 & 0 & -1/C_2 & 0 & 0 & 0 \\ 0 & 0 & 0 & 0 & 0 & 0 & 1/C_3 & 0 & -1/C_3 & -1/C_3 & 0 \\ 0 & 0 & 0 & 0 & 0 & 0 & 0 & 1/C_4 & 0 & 1/C_4 & -1/C_4 \\ 0 & 0 & 1/L_{13} & 0 & -1/L_{13} & 0 & -R_{13}/L_{13} & 0 & 0 & 0 & 0 \\ 0 & 0 & 0 & 1/L_{24} & 0 & -1/L_{24} & 0 & -R_{24}/L_{24} & 0 & 0 & 0 \\ 0 & 0 & 0 & 0 & 1/L_{34} & -1/L_{34} & 0 & 0 & -R_{34}/L_{34} & 0 & 0 \\ -1/L_{35} & 0 & 0 & 0 & 1/L_{35} & 0 & 0 & 0 & 0 & -R_{35}/L_{35} & 0 \\ 0 & -1/L_{46} & 0 & 0 & 0 & 1/L_{46} & 0 & 0 & 0 & 0 & -R_{46}/L_{46} \end{bmatrix}$$

$$\times \begin{bmatrix} e_5 \\ e_6 \\ e_1 \\ e_2 \\ e_3 \\ e_4 \\ i_{13} \\ i_{24} \\ i_{34} \\ i_{35} \\ i_{46} \end{bmatrix} + \begin{bmatrix} -1 & 0 \\ 0 & -1 \\ 0 & 0 \\ 0 & 0 \\ 0 & 0 \\ 0 & 0 \\ 0 & 0 \\ 0 & 0 \\ 0 & 0 \\ 0 & 0 \\ 0 & 0 \end{bmatrix} \begin{bmatrix} i_{g1}^* \\ i_{g2}^* \end{bmatrix} + \begin{bmatrix} 0 & 0 \\ 0 & 0 \\ 1 & 0 \\ 0 & 1 \\ 0 & 0 \\ 0 & 0 \\ 0 & 0 \\ 0 & 0 \\ 0 & 0 \\ 0 & 0 \\ 0 & 0 \end{bmatrix} \begin{bmatrix} i_{w1} \\ i_{w2} \end{bmatrix} \text{ and } Y = \begin{bmatrix} 1 & 0 & 0 & 0 & 0 & 0 & 0 & 0 & 0 & 0 & 0 \\ 0 & 1 & 0 & 0 & 0 & 0 & 0 & 0 & 0 & 0 & 0 \end{bmatrix} \begin{bmatrix} e_5 \\ e_6 \\ e_1 \\ e_2 \\ e_3 \\ e_4 \\ i_{13} \\ i_{24} \\ i_{34} \\ i_{35} \\ i_{46} \end{bmatrix} \quad \text{(A-12)}$$

stabilizes the system DC voltage to the permissible value during the power reduction transition period by the pitch control system. The CCR system is disconnected when wind power is reduced to the new desired values. The droop gain of the healthy grid should be adjusted to sustain the optimal operation.

4. Wind line outage increases the wind farm converter voltage to high values due to a sudden imbalance between the wind power input and the converter DC power output. This voltage instability may lead to losing the whole system. A CCR circuit should also be activated to control the system voltage after the faulty line's disconnection. The CCR circuit should be disconnected after stopping the wind farm's power injection connected to the faulty line. Subsequent update in the droop gains to preserve optimal system operation is necessary.
5. The outage of an interconnecting line does not commonly generate severe voltage instability. However, it may cause overvoltage or overcurrent in the MTDC system, which can be controlled by updating the droop gains.
6. The main problematic outage scenarios can be considered as the wind farm line outage and grid line outage during high wind power injection. These two outages should be treated with care to avoid losing the whole system.

APPENDIX A

Considering the MTDC shown in Fig. 3, the following system equations can be listed using (3) and (4):

Voltage equations

$$C_1\dot{e_1} = i_{w1} - i_{13} \tag{A-1}$$
$$C_2\dot{e_2} = i_{w2} - i_{24} \tag{A-2}$$
$$C_3\dot{e_3} = i_{13} - i_{35} - i_{34} \tag{A-3}$$
$$C_4\dot{e_4} = i_{24} + i_{35} - i_{46} \tag{A-4}$$
$$C_5\dot{e_5} = i_{35} - i_{g1} \tag{A-5}$$
$$C_6\dot{e_6} = i_{46} - i_{g2} \tag{A-6}$$

Current equations

$$L_{13}\dot{i_{13}} = e_1 - e_3 - R_{13}i_{13} \tag{A-7}$$
$$L_{24}\dot{i_{24}} = e_2 - e_4 - R_{24}i_{24} \tag{A-8}$$
$$L_{34}\dot{i_{34}} = e_3 - e_4 - R_{34}i_{34} \tag{A-9}$$
$$L_{35}\dot{i_{35}} = e_3 - e_5 - R_{35}i_{35} \tag{A-10}$$
$$L_{46}\dot{i_{46}} = e_4 - e_6 - R_{46}i_{46} \tag{A-11}$$

Then the state-space model can be depicted as follows (A-12), as shown at the bottom of the previous page.

REFERENCES

[1] F. D. Bianchi, J. L. Domínguez-García, and O. Gomis-Bellmunt, "Control of multi-terminal HVDC networks towards wind power integration: A review," *Renew. Sustain. Energy Rev.*, vol. 55, pp. 1055–1068, Mar. 2016.
[2] M. Aragüés-Peñalba, A. Egea-Àlvarez, S. G. Arellano, and O. Gomis-Bellmunt, "Droop control for loss minimization in HVDC multi-terminal transmission systems for large offshore wind farms," *Electr. Power Syst. Res.*, vol. 112, pp. 48–55, Jul. 2014.
[3] A. E. B. Abu-Elanien, A. A. Elserougi, A. S. Abdel-Khalik, A. M. Massoud, and S. Ahmed, "A differential protection technique for multi-terminal HVDC," *Electr. Power Syst. Res.*, vol. 130, pp. 78–88, Jan. 2016.
[4] A. E. B. Abu-Elanien, A. S. Abdel-Khalik, A. M. Massoud, and S. Ahmed, "A non-communication based protection algorithm for multi-terminal HVDC grids," *Electr. Power Syst. Res.*, vol. 144, pp. 41–51, Mar. 2017.
[5] A. Raza, A. Akhtar, M. Jamil, G. Abbas, S. O. Gilani, L. Yuchao, M. N. Khan, T. Izhar, X. Dianguo, and B. W. Williams, "A protection scheme for multi-terminal VSC-HVDC transmission systems," *IEEE Access*, vol. 6, pp. 3159–3166, Dec. 2017.
[6] L. Liu, Z. Liu, M. Popov, P. Palensky, and M. A. M. M. van der Meijden, "A fast protection of multi-terminal HVDC system based on transient signal detection," *IEEE Trans. Power Del.*, vol. 36, no. 1, pp. 43–51, Feb. 2021.
[7] W. Wang, M. Barnes, O. Marjanovic, and O. Cwikowski, "Impact of DC breaker systems on multiterminal VSC-HVDC stability," *IEEE Trans. Power Del.*, vol. 31, no. 2, pp. 769–779, Apr. 2016.
[8] A. E. B. Abu-Elanien, A. S. Abdel-Khalik, A. M. Massoud, and S. Ahmed, "Design of optimal droop control for multi-terminal high-voltage direct current systems during line outages," *Electr. Power Compon. Syst.*, vol. 47, nos. 9–10, pp. 772–784, Jun. 2019.
[9] X. Chen, L. Wang, H. Sun, and Y. Chen, "Fuzzy logic based adaptive droop control in multiterminal HVDC for wind power integration," *IEEE Trans. Energy Convers.*, vol. 32, no. 3, pp. 1200–1208, Sep. 2017.
[10] A. A. Jamshidi Far, D. Jovcic, and A. M. Alsseid, "DC voltage droop gain for a five-terminal DC grid using a detailed dynamic model," *Int. Trans. Electr. Energy Syst.*, vol. 26, no. 2, pp. 429–443, Feb. 2016.
[11] Y. Che, J. Jia, J. Zhu, X. Li, Z. Lv, and M. Li, "Stability evaluation on the droop controller parameters of multi-terminal DC transmission systems using small-signal model," *IEEE Access*, vol. 7, pp. 103948–103960, 2019.
[12] L. Xiao, Z. Xu, T. An, and Z. Bian, "Improved analytical model for the study of steady state performance of droop-controlled VSC-MTDC systems," *IEEE Trans. Power Syst.*, vol. 32, no. 3, pp. 2083–2093, May 2017.
[13] M. Aragüés-Peñalba, A. Egea-Àlvarez, O. Gomis-Bellmunt, and A. Sumper, "Optimum voltage control for loss minimization in HVDC multi-terminal transmission systems for large offshore wind farms," *Electr. Power Syst. Res.*, vol. 89, pp. 54–63, Aug. 2012.
[14] A. S. Abdel-Khalik, A. M. Massoud, A. A. Elserougi, and S. Ahmed, "Optimum power transmission-based droop control design for multi-terminal HVDC of offshore wind farms," *IEEE Trans. Power Syst.*, vol. 28, no. 3, pp. 3401–3409, Aug. 2013.
[15] J. Khazaei, Z. Miao, L. Piyasinghe, and L. Fan, "Minimizing DC system loss in multi-terminal HVDC systems through adaptive droop control," *Electr. Power Syst. Res.*, vol. 126, pp. 78–86, Sep. 2015.
[16] S. Sayed and A. Massoud, "Minimum transmission power loss in multi-terminal HVDC systems: A general methodology for radial and mesh networks," *Alexandria Eng. J.*, vol. 58, no. 1, pp. 115–125, Mar. 2019.
[17] J. Beerten and R. Belmans, "Analysis of power sharing and voltage deviations in droop-controlled DC grids," *IEEE Trans. Power Syst.*, vol. 28, no. 4, pp. 4588–4597, Nov. 2013.
[18] Y. Wen, J. Zhan, C. Y. Chung, and W. Li, "Frequency stability enhancement of integrated AC/VSC-MTDC systems with massive infeed of offshore wind generation," *IEEE Trans. Power Syst.*, vol. 33, no. 5, pp. 5135–5146, Sep. 2018.
[19] H. Dong, Z. Xu, P. Song, G. Tang, Q. Xu, and L. Sun, "Optimized power redistribution of offshore wind farms integrated VSC-MTDC transmissions after onshore converter outage," *IEEE Trans. Ind. Electron.*, vol. 64, no. 11, pp. 8948–8958, Nov. 2017.
[20] A. Yogarathinam and N. R. Chaudhuri, "Stability-constrained adaptive droop for power sharing in AC-MTDC grids," *IEEE Trans. Power Syst.*, vol. 34, no. 3, pp. 1955–1965, May 2019.
[21] G. Grdenić and M. Delimar, "Small-signal stability analysis of interaction modes in VSC MTDC systems with voltage margin control," *Energies*, vol. 10, no. 7, p. 873, Jun. 2017.
[22] W. Liu, B. Qin, R. Zhang, J. Liu, and H. Li, "Impact of control system on small-signal stability of MMC-based MTDC transmission system," *Energy Rep.*, vol. 6, pp. 1130–1135, Dec. 2020.

[23] S. Sayed and A. Massoud, "Impact of forced and unforced system parameter variations on network stability and system economics of radial MTDC networks," *Electr. Power Syst. Res.*, vol. 179, pp. 1–10, Feb. 2020, Art. no. 106051.
[24] W. Wang, M. Barnes, and O. Marjanovic, "Stability limitation and analytical evaluation of voltage droop controllers for VSC MTDC," *CSEE J. Power Energy Syst.*, vol. 4, no. 2, pp. 238–249, Jun. 2018.
[25] D. Tzelepis, A. O. Rousis, A. Dyśko, C. Booth, and G. Strbac, "A new fault-ride-through strategy for MTDC networks incorporating wind farms and modular multi-level converters," *Int. J. Electr. Power Energy Syst.*, vol. 92, pp. 104–113, Nov. 2017.
[26] K. Shinoda, A. Benchaib, J. Dai, and X. Guillaud, "Over- and under-voltage containment reserves for droop-based primary voltage control of MTDC grids," *IEEE Trans. Power Del.*, early access, Jan. 25, 2021, doi: 10.1109/TPWRD.2021.3054183.
[27] W. Du, Q. Fu, and H. Wang, "Damping torque analysis of DC voltage stability of an MTDC network for the wind power delivery," *IEEE Trans. Power Del.*, vol. 35, no. 1, pp. 324–338, Aug. 2020.
[28] L. Jun, J. Tianjun, O. Gomis-Bellmunt, J. Ekanayake, and N. Jenkins, "Operation and control of multiterminal HVDC transmission for offshore wind farms," *IEEE Trans. Power Del.*, vol. 26, no. 4, pp. 2596–2604, Oct. 2011.
[29] A. S. Abdel-Khalik, A. E. B. Abu-Elanien, A. A. Elserougi, S. Ahmed, and A. M. Massoud, "A droop control design for multiterminal HVDC of offshore wind farms with three-wire bipolar transmission lines," *IEEE Trans. Power Syst.*, vol. 31, no. 2, pp. 1546–1556, Mar. 2016.
[30] S. Sanchez, A. Garcés, G. Bergna-Diaz, and E. Tedeschi, "Dynamics and stability of meshed multiterminal HVDC networks," *IEEE Trans. Power Syst.*, vol. 34, no. 3, pp. 1824–1833, May 2019.
[31] L. Xu and L. Yao, "DC voltage control and power dispatch of a multi-terminal HVDC system for integrating large offshore wind farms," *IET Renew. Power Gener.*, vol. 5, no. 3, pp. 223–233, May 2011.
[32] N. Chaudhuri, B. Chaudhuri, R. Majumder, and A. Yazdani, *Multi-Terminal Direct-Current Grids: Modeling, Analysis, and Control*, 1st ed. Hoboken, NJ, USA: Wiley, 2014.
[33] J. Yang, J. E. Fletcher, and J. O'Reilly, "Short-circuit and ground fault analyses and location in VSC-based DC network cables," *IEEE Trans. Ind. Electron.*, vol. 59, no. 10, pp. 3827–3837, Oct. 2012.
[34] S. K. Chaudhary, R. Teodorescu, P. Rodriguez, and P. C. Kjar, "Chopper controlled resistors in VSC-HVDC transmission for WPP with full-scale converters," in *Proc. IEEE PES/IAS Conf. Sustain. Alternative Energy (SAE)*, Valencia, Spain, Sep. 2009, pp. 1–8.
[35] B. Silva, C. L. Moreira, H. Leite, and J. A. P. Lopes, "Control strategies for AC fault ride through in multiterminal HVDC grids," *IEEE Trans. Power Del.*, vol. 29, no. 1, pp. 395–405, Feb. 2014.

AHMED E. B. ABU-ELANIEN (Senior Member, IEEE) received the B.Sc. and M.Sc. degrees in electrical engineering from Alexandria University, Alexandria, Egypt, in 2001 and 2006, respectively, and the Ph.D. degree from the University of Waterloo, Waterloo, ON, Canada, in 2011.

From June 2011 to November 2012, he was a Postdoctoral Fellow with the Department of Electrical and Computer Engineering, University of Waterloo. From December 2012 to August 2016, he was an Assistant Professor with the Electrical Engineering Department, Faculty of Engineering, Alexandria University. From September 2016 to August 2020, he was an Assistant Professor with the Electrical and Computer Engineering Department, Dhofar University, Salalah, Oman. He is currently an Associate Professor with the Electrical Engineering Department, Faculty of Engineering, Alexandria University. His research interests include HVDC, protection, smart grids, and asset management.

Dr. Abu-Elanien is a member of IET. He is an Associate Editor of the *Alexandria Engineering Journal*.

AYMAN S. ABDEL-KHALIK (Senior Member, IEEE) received the B.Sc. and M.Sc. degrees in electrical engineering from Alexandria University, Alexandria, Egypt, in 2001 and 2004, respectively, and the Ph.D. degree in electrical engineering from Alexandria University, and Strathclyde University, Glasgow, U.K., in 2009, under a dual-channel program. He is currently a Professor with the Electrical Engineering Department, Faculty of Engineering, Alexandria University. His current research interests include electrical machine design and modeling, electric drives, energy conversion, and renewable energy. He serves as an Associate Editor for IEEE TRANSACTIONS ON INDUSTRIAL ELECTRONICS and *IET Electric Power Applications Journal* and an Executive Editor of *Alexandria Engineering Journal*.

AHMED M. MASSOUD (Senior Member, IEEE) received the B.Sc. (Hons.) and M.Sc. degrees in electrical engineering from Alexandria University, Egypt, in 1997 and 2000, respectively, and the Ph.D. degree in electrical engineering from Heriot-Watt University, Edinburgh, U.K., in 2004. He is currently the Associate Dean of Research and Graduate Studies with the College of Engineering and a Professor in electrical engineering with the College of Engineering, Qatar University. He holds eight U.S. patents. He published more than 100 journal articles in power electronics, energy conversion, and power quality. His research interests include power electronics, energy conversion, renewable energy, and power quality.